PERFORMANCE COMPARISON BETWEEN ADAPTIVE LINE ENHANCER AND FFT FOR FAST CARRIER ACQUISITION

Hen-Geul Yeh and T. M Nguyen

Jet Propulsion Laboratory
California Institute of Technology
4800 Oak Grove Drive
Pasadena, CA 91109-8099

been proposed in the literature to solve such problems. These methods provide excellent results but may require excessively long time observations because of batch processing.

Recently, time-domain spectra] estimation techniques based on adaptive line enhancer (A LE) are introduced [4-9]. The adaptive line enhancement system is depicted in Figure I (b). The system, which was introduced by Widrow [5], uses the measured signal as desired response and a delayed version of itself as input. The principle is that the delay should decorrelate the noise between the primary and reference inputs while leaving the narrowband carrier signal correlated. When functioning in an ideal way, the adaptive filter output is an enhanced version of the carrier components with higher CNR. Both CNR and SNR are used in this paper and they are interchangeable.

The adaptive filter depicted in Figure 1 (b) is a time-varying system and the weight vector is updated based on the Least Mean Squares (LMS) algorithm. The LMS algorithm is derived based on the method of steepest descent [5]. There are many applications have been developed by using the LMS algorithm. The fast measurement of digital instantaneous frequency [6] is one of the applications. In addition, it is well-known that the LMS type algorithms are more robust to sudden variation of the environment parameters than the FFT.

The ALE algorithm and architecture for fast acquisition are presented in this paper. The general properties of an ALE is discussed in Section 2. Simulations for acquiring fixed frequency and sweeping signals are provided in Section 3. Performance comparison between FFT and ALE is also discussed is Section 3. Conclusion is given in Section 4.

2. *THE ALE ALGORITHM*

The ALE architecture is shown in Figure 1 (b). The ALE algorithm is given as follows:

$$y_k = W_k^T X_{k-m}$$ (2.1)

where $X_k = [x_k \ x_{k-1} \ . \ . \ . \ x_{k-L}]^T$
$$W_k = [w_0 \ w, \ . \ . \ . \ w_L]^T.$$

The error sequence is defined as

$$e_k = x_k - y_k.$$ (2.2)

The weight vector is updated as follows:

$$w_{k+1} = W_k + 2\mu e_k X_{k-m}$$ (2.3)

where μ is the step size of the adaptation

The convergence of the weight vector is assured by [5]:

$$0 \prec \mu \prec \frac{1}{(L + 1)(carrier + noise\ power)} \qquad (2.4)$$

where $L+1$ is the number of taps of the adaptive filter. The optimal Weight vector W_{opt}, called the Wiener weight vector, is found in [5] as

$$W_{opt} = R^{-1} P \qquad (2.5)$$

where

$$R = E[X_{k-m} X_{k-m}^{T}] = R_s + R_n \qquad (2,6)$$

where R_s = autocorrelation matrix of the carrier component and R_n = autocorrelation matrix of the noise with power σ_n^2, and

$$P = E[X_{k-m} x_k]. \qquad (2.7)$$

The input signal vector to the adaptive filter is X_{k-m}, where m is the delay units. The delay unit m chosen must be of sufficient length to cause the broadband noise components in the filter (reference) input to become uncorrelated from those in the primary input The carrier signal components, because of their periodic nature, will remain correlated with each other.

The optimal linear solution for selecting the weight vector of an ALE is similar to the so-called matched filter. For a carrier at frequency ω_0 embedded in white noise, the matched filter response is a sampled sinusoidal signal whose frequency is ω_0. The matched filter produces the peak SNR at each sample, but does not preserve the carrier signal waveform at the output, especially when the input signal has time-varying parameters. The matched filter solution dots provide the best SNR gain obtainable by linear processing. However, the solution can only be constructed by giving prior knowledge of the frequency ω_0. On the other hand, the ALE output y_k preserves the carrier signal waveform. Furthermore, it is not necessary to have a priori knowledge of the received signal parameters, such as carrier SNR, Doppler and carrier sweeping rate. For example, the carrier frequency sweeping rate depends on the uplink carrier signal level for deep space mission. The uplink carrier frequency ω_0 sweeping rate is set to about 544 and 40 Hz/sec around the best lock frequency when the carrier signal level is equal to -110 and -151 dBm, respectively. Therefore, the ALE method is a technique designed to approximate the optimal SNR gain obtained by the matched filter sohrtion for this problem.

This ALE system output CNR is then obtained as follows:

3

$$CNR_{out} = \frac{output\ carrier\ power}{output\ noise\ power} = \frac{E[y_s^2(k)]}{E[y_n^2(k)]} = \frac{(L+1)a^2}{\sigma_n^2} \qquad (2.8)$$

The ALE system input CNR power ratio is

$$CNR_{input} = \frac{input\ carrier\ power}{input\ noise\ power} = \frac{a^2}{\sigma_n^2} \qquad (2.9)$$

Therefore, the ALE optimal steady state CNR gain is

$$G_{ALE} = \frac{CNR_{output}}{CNR_{input}} = L + 1 \qquad (2.10)$$

Equation (2, 10) shows that the ALE optimal CNR gain is proportional to the length of the adaptive filter

3. SIMULATIONS

The detectability of a CW signal in white Gaussian noise by using the ALE and FFT is studied via simulations at same CNRS for comparison. Several simplified cases for a deep space transponder uplink CW detection arc simulated. The time constant and number of weights of ALE are selected so that both the FFT and the ALE will have the same frequency resolution and will usc the same amount of input data samples, allowing a critical but fair comparison between the.sc approaches. Delay parameter m is chosen as 1. The second IF bandwidth is assumed to be 64 kIIz. These parameters arc used for all simulations except the case B.3 where the 2nd 1 F bandwidth employed is 32 kHz.

Case A. Fixed CW Frequency.

The carrier signal is a sinusoidal with a fixed frequency and the samplii ig rate is 8 t imcs the carrier frequency. In this case, three different unlink CNRS are provided; the corresponding second IF CNRS and optimal number of taps of ALE are calculated for simulations.

Case A. 1. The transponder received uplink signal level is -133 dBm and the corresponding second IF CNR is equal to -9 dB. The optimal number of weights is 16 of the ALE. This is a low-frequency resolution case. The total number of data samples used is 32768. The step size is chosen as O. 125/32768. The FFT is the average of 2048 transforms, each with 16 points. Figures 2 (a)-(b) present the carrier detector plots obtained by using the ALE and FFT, respectively. Figure 2 (a) shows the transfer function magnitude of the ALE. Figure 2(b) shows the power spectral density (squared magnitude of FFT/16^2). Visual examination indicates that the FFT provides a higher peak for CW detection than the ALE.

Case A.2. The transponder received signal level is -142 dBm and the corresponding second IF CNR is equal to -18 dB. The optimal number of weights is 128 of the ALE. This is a medium-frequency resolution case. The number of input samples is selected as 32768. The step size is chosen as 0.015625/32768. The FFT is the average of 256 transforms, each with 128 points. Figures 3 (a)-(b) present the carrier detector plots obtained by using the ALE and FFT, respectively. Figure 3 (a) shows the transfer function magnitude of the ALE. Figure 3(b) shows

the power spectral density by using FFT. Visual examination indicates that the FFT provides a higher peak for CW detection than the ALE.

Case A.3. The transponder received signal level is -151 dBm and the corresponding second IF CNR is equal (o -27 dB. The optimal number of weights is 1024 of the AI .E. This is a high-frequency resolution case. The number of input samples is selected as 4*32768. The step size is chosen as 1/(5 12*32768). The FFT is the average of 128 transforms, each with 1024 points. Four weight vectors are averaged, each vector is taken at the end of the 32768 data samples Figures 4(a)-(b) present the carrier detector plots obtained by using the ALE and FFT, respectively. Figure 4(a) shows the averaged transfer function magnitude of the AI.11. Figure 4(b) shows the power spectral density by using FFT. Visual examination indicates that the FFT provides a higher peak for CW detection than the ALE.

Case B. Swept CW Frequency

The uplink carrier signal is swept from the best lock frequency and the sampling rate is fixed at 10 kHz which is 8 times the down converted CW frequency. in this case, three different CNRS are provided and the corresponding sweeping rates are employed to generate uplink C W signals.

Case B. 1. The CNR of this case is the same as that of Case A. 1 except (he uplink CW is swept at 352 Hz/sec. All design parameters used for this case is the same as that of case A. 1. Again, this is a low-frequency resolution case. Figures 5(a)-(b) present the carrier detector plots obtained by using the ALE and FFT, respectively. Figure 5(a) shows the transfer function magnitude of the ALE. Figure 5(b) shows the power spectral density. At the end of 32768 input samples, the carrier frequency is swept from 1250 to 2403 Hz. The ALE plot provides the highest signal peak around 2500 Hz, which is offset about 100 Hz, as shown in Figure 5(a). However, the FFT plot shows a peak around 1875 Hz which is offset about 625 Hz. Visual examination indicates that the ALE output provides better earl-icr signal detection than FFT.

Case B.2. The CNR of this case is the same as that of Case A.2 except the uplink CW is swept at 96 Hz/see. All design parameters used for this case is the same as that of case A.2 except that two weight vectors are averaged (two input data sets), each vector is taken at the end of the 32768 data samples; and FFT is the average of 512 transforms, each with 128 points. At the end of 32768 input samples, the carrier frequency is swept from 1250 to 1565 Hz. The ALE plot provides the highest signal peak around 1563 Hz as shown in Figure 6(a). However, the FFT plot shows a wide-band pulse from 1250 to 1563 Hz. This is simply because that FFT detects the complete frequency range where the carrier swept through. Visual examination indicates that the ALE provides better carrier signal detection than FFT.

Case B.3. The CNR of this case is the same as that of Case A.3 except the uplink CW is swept at 40 Hz/sec and the 2nd IF bandwidth is reduced from 64 to 32 kHz. The corresponding 2nd IF CNR is equal to -24 dB. All design parameters used for this case is the same as that of case A.3 except that 32*32768 data samples are employed. Thirty-t wo weight vectors are averaged, each vector is taken at the end of the 32768 data samples; and FFT is the average of 1024 transforms, each with 1024 points. At the end of 32768 input samples, the carrier frequency is swept from 1250 to 1381 Hz. The ALE plot provides the highest signal peak around 1380 Hz as shown in Figure 7(a). However, the FFT plot shows a wide-barrd pulse from 1250 to 1380 Hz. This is simply because that FFT detects the complete frequency range where the carrier swept through. Visual examination indicates that the ALE provides better carrier signal detection than FFT. These simulation results are agreed with [10] very well.

Note that the sampling frequency selected and the sweeping rate used here have an important effect on the carrier detection. The sweeping rates used in here are the typical values currently employed for deep space missions, If the sampling frequency is greater than 100 kHz, the Figure 5 will be look like Figure 2 due to the fact that the frequency increment is relatively too small. Consequently, both cases A and B will provide similar results. Furthermore, both the bandwidth of the 2nd IF signal and the total number of data samples are also important factors on the carrier detection for fast acquisition. The narrower bandwidth of the 2nd IF signal (i.e. the higher CNR at 2nd 1 F), the less total number of data samples are needed for a fast and accurate carrier detection. However, the bandwidth of the 2nd IF signal can't be less than 32 kHz, because the subcarrier of Command Detection Unit (CDU) is located at 16 kHz away from the center frequency of the bandpass filter.

4. *CONCLUSION*

In this paper, the detectability of a CW signal in white Gaussian noise by using the ALE and FFT was studied via simulations at same CNRS for comparison. Both fixed and swept uplink C W cases were simulated for a deep space transponder application. '1 'he time constant and number of weights of ALE were selected so that both the FFT and the ALE had the same frequency resolution and would use the same amount of input data samples, allowing a critical but fair comparison between these approaches. In the fixed uplink CW case, the carrier detection by using FFT is better than that of ALE. On the other hands, the carrier detection by using ALE is better than that FFT in the swept uplink CW case. Consequently, the ALE is recommended for deep space transponder for fast carrier acquisition during sweeping uplink CW signal

ACKNOWLEDGEMENT

REFERENCES

1. S. Acquirre, D. H. Brown, and W. J. Hurd, "Phase lock acquisition for sampled data PLLs using the sweep technique," TDA Progress Report 42-86, pp. 95-102, April-June, 1986.
2. B. Shah and S. Hinedi, "A comparison of open-loop frequency acquisition techniques for suppressed carrier biphase signals," TDA Progress Report 42-103, July -Sep., 1990.
3. M. Aung, et al., "Block V receiver fast acquisition algorithm for the Galileo S-band miss ion," will be published in TDA Progress Report.
4. H. G. Ych and T. M. Nguyen, "Adaptive line enhancers for fast acquisition," TDA Progress Report 42-119, pp. 140-159, Nov., 1994.
5. B. Widrow et al., "Adaptive noise canceling principles and applications," Proc. IEEE, vol. 63, pp. 1692-1716, Dec. 1975.
6. L. Griffiths, "Rapid measurement of digital instantaneous frequency," IEEE Trans. Acoust., Speech, Signal Processing, Vol. ASSP-23, No. 2, pp. 207-222, April 1975. '
7. J. R. Zeidler and D. M. Chabries, "An analysis of the LMS adaptive filter used as a spectral line enhancer," Naval Undersea Center, Tech. Note 1476, Feb. 1975.
8. W. S. Burdic, "Detection of narrow-band signals using time-domain adaptive filter," IEEE Trans. Acrosp. Electron. Syst., vol. AES-14, pp. 578-591, July 1978.
9. J. T. Richard et al., "A performance analysis of adaptive line enhancer - augmented spectral detectors," IEEE Trans. ASSP, vol. ASSP-29, pp.694-701, June 1981.
10 D. W. Tufts ct al., "Adaptive line enhancement and spectrum analysis," Proc. of IEEE Letter, pp. 169-173, Jan. 1977.

Figure 1. The block diagram of using ALE in the digital receiver for both acquisition and tracking.
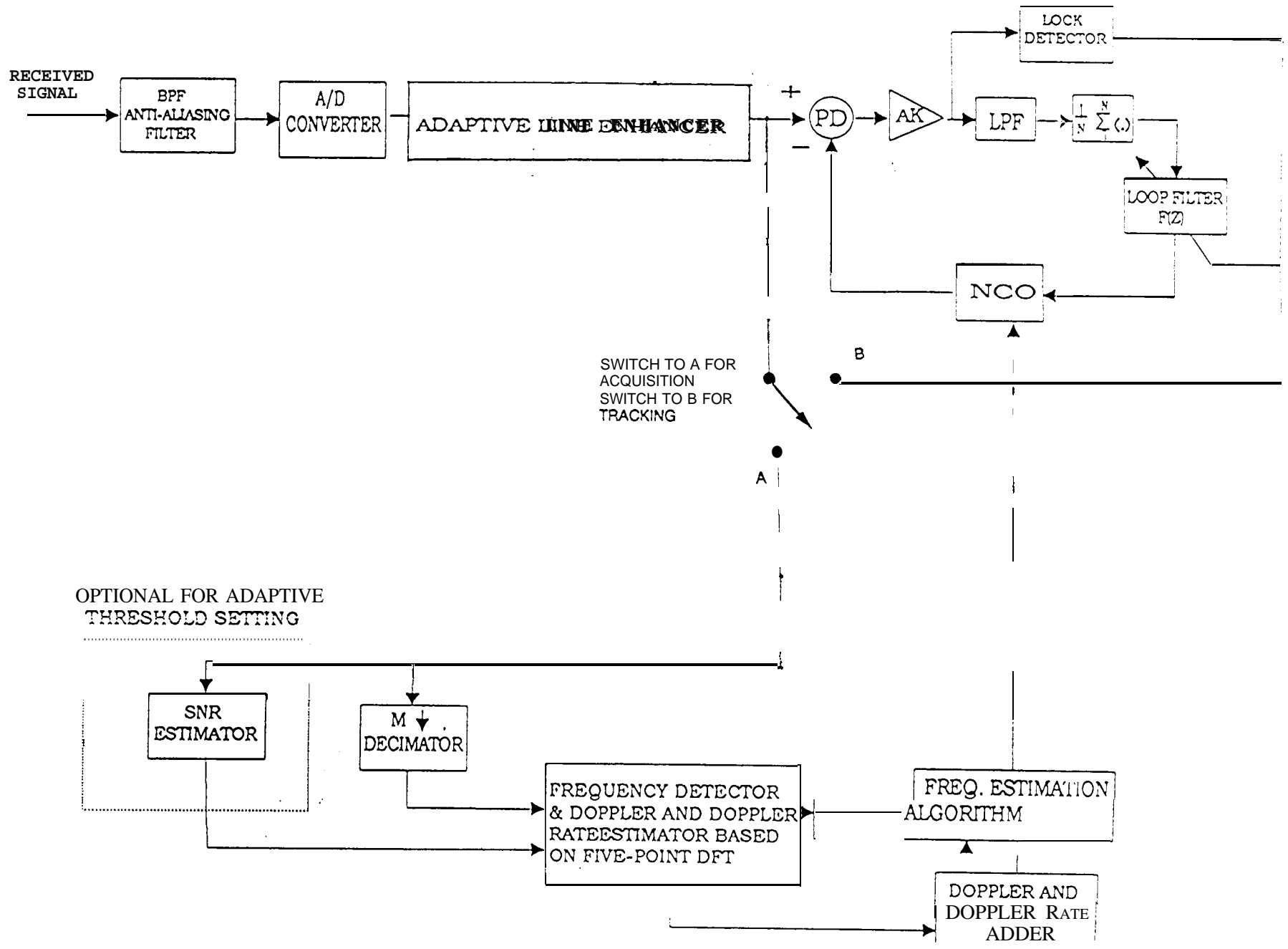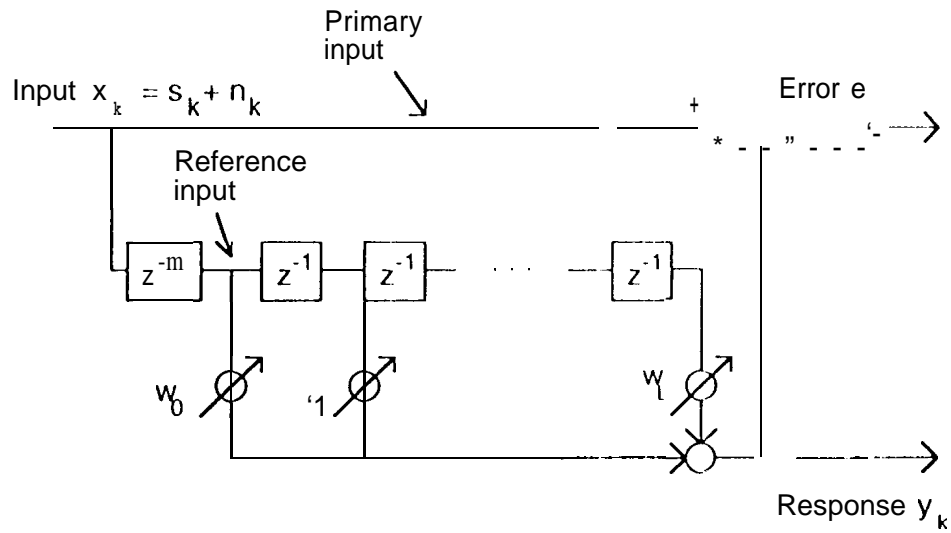
Figure 1(b). The structure of the conventional adaptive line enhancer
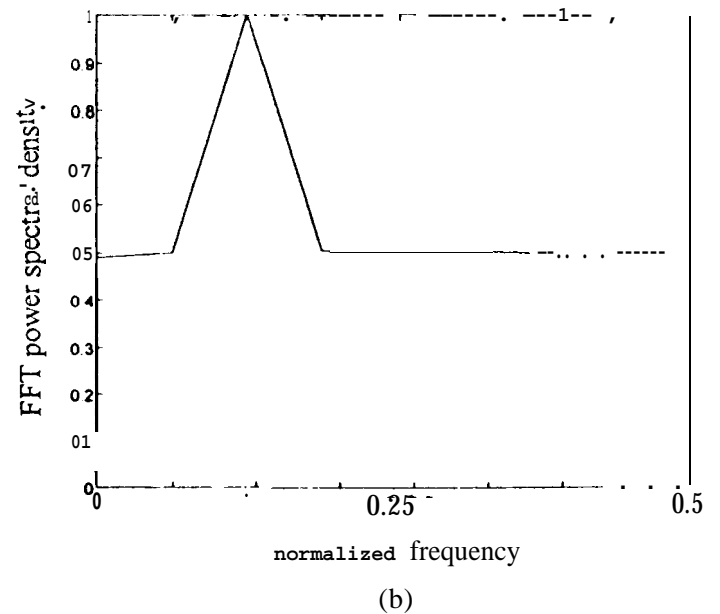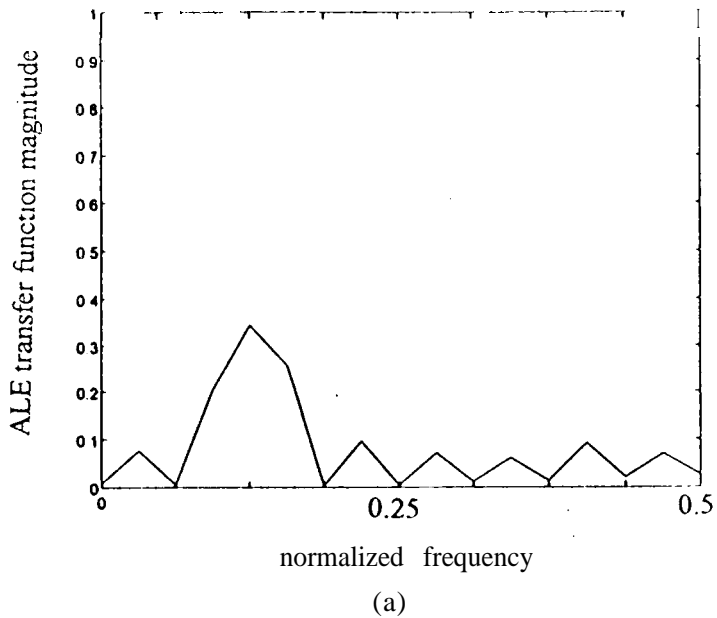

(a)

(b)

Figure 2. Case A. 1: Carrier detector plots with low frequency resolution (16-point)@ fixed uplink
frequency at signal level -133 dBm, (a) magnitude of the ALE transfer function, (b) power
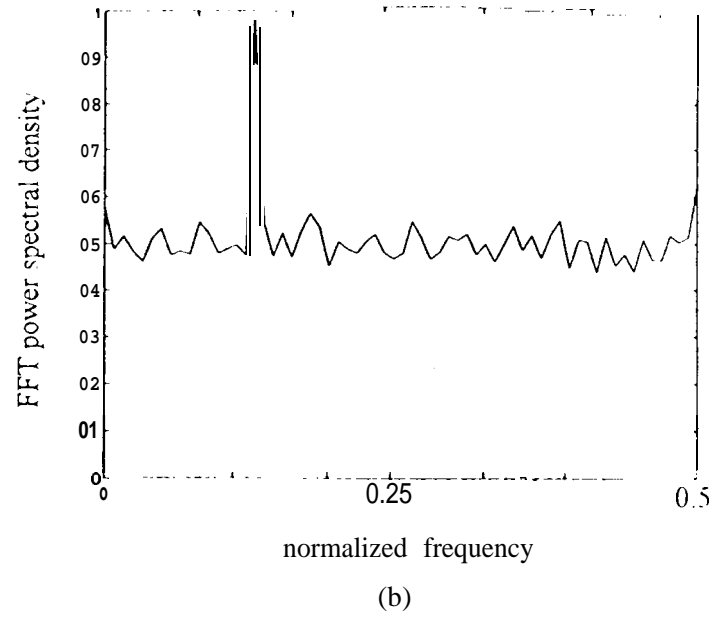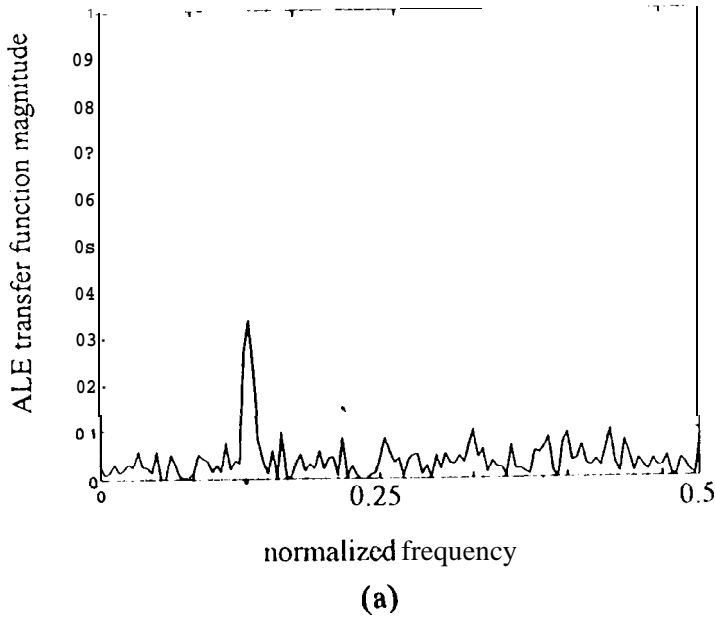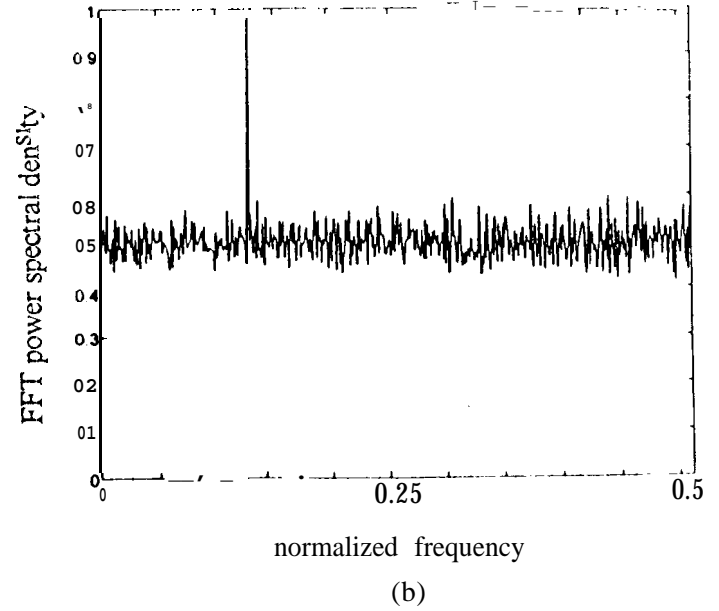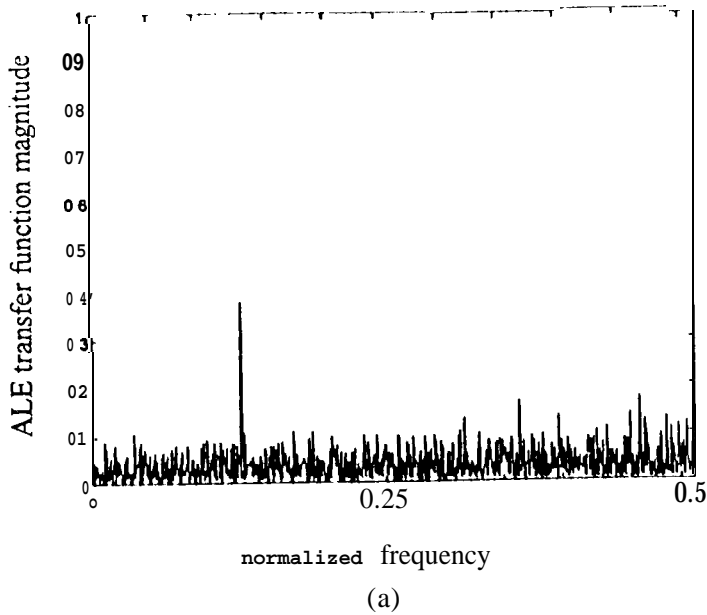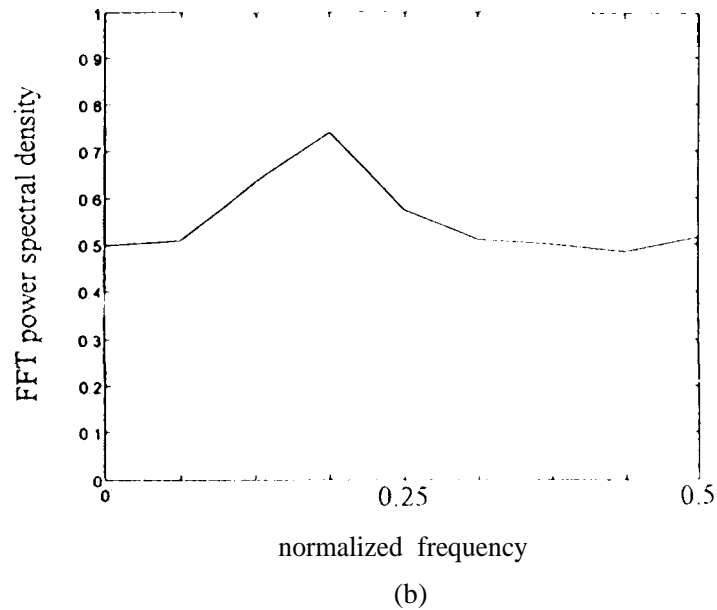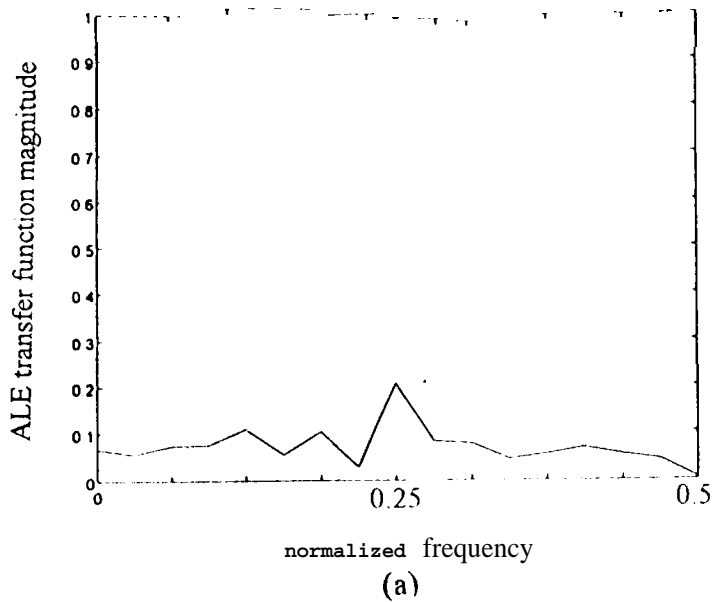spectra! density of the 16-point FFT.

Figure 3. Case A.2: Carrier detector plots with medium frequency resolution (128-point) @ fixed uplink frequency at signal level -142 dBm, (a) magnitude of the ALE transfer function, (b) power spectral density of the 128-point FFT.

Figure 4. Case A.3: Carrier detector plots with medium frequency resolution (1024-point)@, fixed uplink frequency at signal level -151 dBm, (a) magnitude of the ALE transfer function, (b) power spectral density of the 128-point FFT.

Figurc 5. Case B.1: Carrier dctcctor plots with low frcqucncy resolution (16-point), uplink frequcncy sweep rate = 352 Hz/sec at signal level -133 dBm, (a) magnitude of the ALE transfer function, (b) power spectral density of the 128-point FFT.
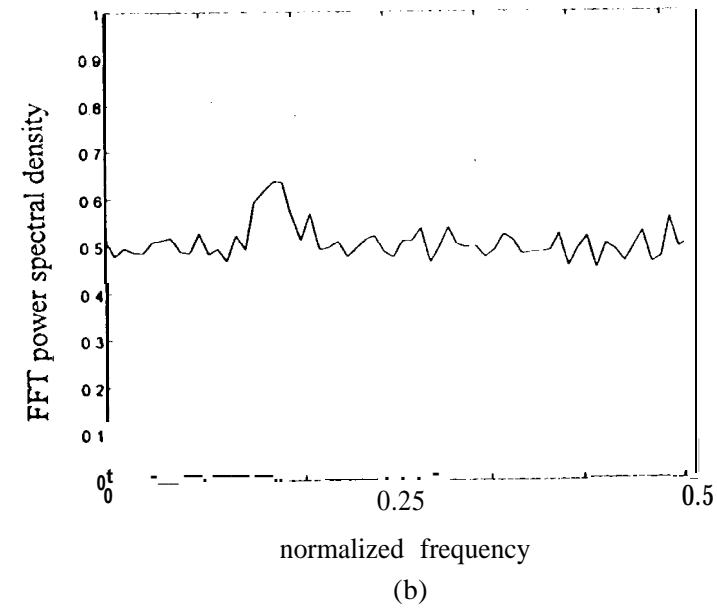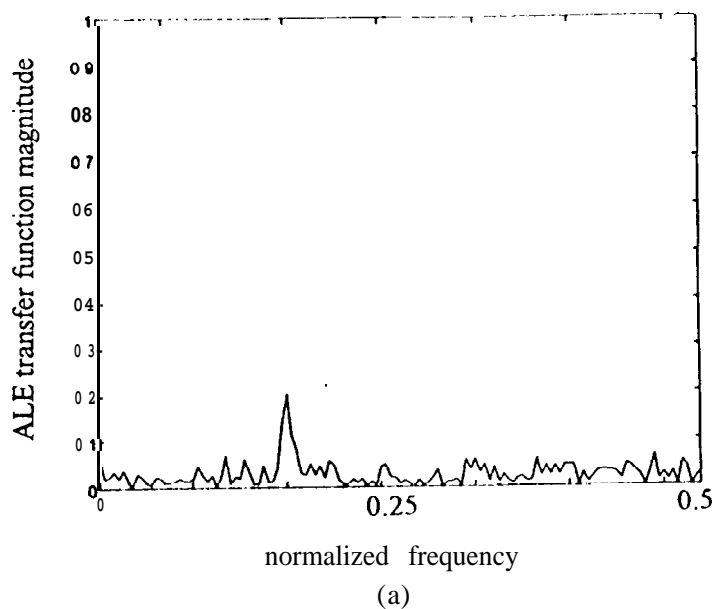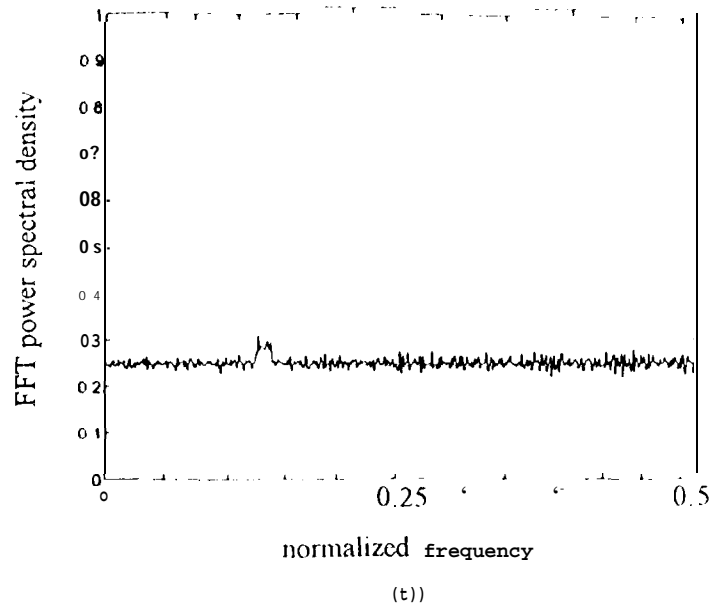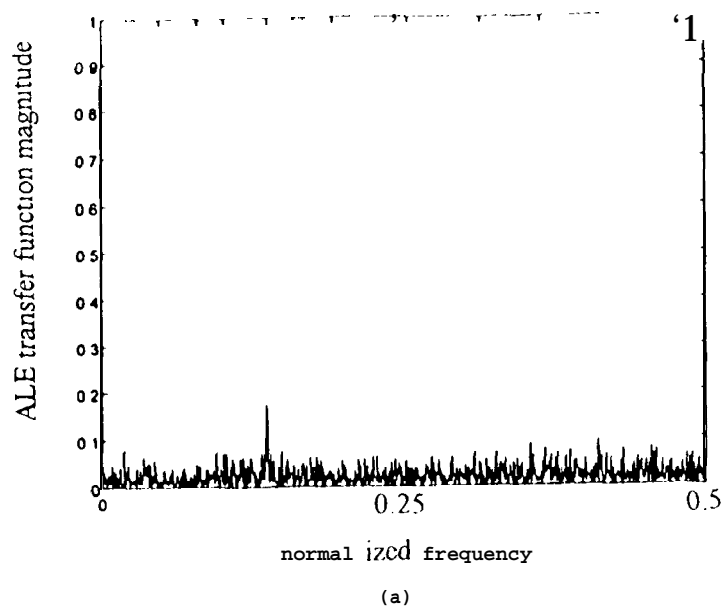

Figure 6. Case B.2: Carrier detector plots with medium frequency resolution (1 28-point), uplink frequency sweep rate ‾96 Hz/sec at signal level -142 dBm, (a) magnitude of the ALE transfer function, (b) power spectral density of the 128-point FFT.

Figure 7. Case 13.3: **Carrier** detector plots with high frequency resolution (1024-point), uplink frequency sweep rate = 40 Hz/sec at signal level -151 dBm, but 2nd IF bandwidth = 32 kHz; (a) magnitude of the ALE transfer function, (b) power spectral density of the 1024-point FIT.